DOI: 10.17344/acsi.2023.8005 *Acta Chim. Slov.* **2023,** *70,* 310–317

Scientific paper

Preparation, Structure, Characterization and Properties of a Novel $[Y(HIA)_3(H_2O)_2]n \cdot nYCl_3$ (HIA = Isonicotinic Acid)

Kun-Zhong Yang,[1,3] Rong Zou,[1] Wen-Ming Liao,[1] Xiu-Guang Yi[1,*] and Jin-Bing Zhang[2,*]

[1] *School of Chemistry and Chemical Engineering, Jinggangshan University, Ji'an, 343009, China*

[2] *School of Materials Science and Engineering, NingboTech University, Ningbo, 315100, China*

[3] *Experimental Testing Team of Jiangxi Geological Bureau, Nanchang, 330009, China*

** Corresponding author: E-mail: jayxgggchem@163.com & zhangjb@nbt.edu.cn*

Received: 01-08-2023

Abstract

A novel yttrium complex $[Y(HIA)_3(H_2O)_2]_n \cdot nYCl_3$ (HIA = isonicotinic acid) has been synthesized via a hydrothermal reaction and characterized by single crystal X-ray diffraction technique. The title complex features a one-dimensional (1-*D*) chain-like structure. A solid state photoluminescence measurement revealed that there is one strong emission peak at 487 nm. These peak can be assigned to the characteristic electronic transition and stacking effect inside the ligand. The title complex shows CIE (Commission Internationale de I' Éclairage) chromaticity coordinates in the blue region (0.1049, 0.1221). At the same time, the title complex has a wide band gap of 2.03 eV, which was revealed by a solid-state UV/Vis diffuse reflection experiment.

Keywords: Yttrium, Crystal structure, Photoluminescence, Band gap

1. Introduction

In recent decades, lanthanide coordination complexes have attracted more and more interest, due to their excellent photoluminescence properties, magnetic and other properties. [1–5] At present, lanthanide coordination complexes have been found to be widely used in luminescent probes, electroluminescent devices, luminescent materials, magnetic materials, cell imaging and sensors.[6–10] It is well known that the chemical and physical properties of lanthanide coordination complexes are mainly related to the 4*f* electronic configuration of rare earth ions. For example, if 4*f* electrons in lanthanide coordination complexes are effectively transferred, photoluminescence may occur. However, in many cases, due to the low absorption coefficient of rare earth ions, the conversion between 4*f* election orbitals is impossible to form, so lanthanide coordination complexes usually cannot show ideal photoluminescence. In order to increase the absorption coefficient of rare earth ions and promote the conversion between 4*f* electron orbitals, scientists usually a strategy called "antenna effect". In order to achieve this strategy, scientists usually use organic molecular ligands with conjugated structure as "antenna" effect to bind rare earth ions.[11–13]

Aromatic carboxylic acid is a good organic ligand, and its carboxylate ion has a variety of ligand modes, such as monodentate coordination, symmetrical chelation coordination, asymmetrical chelation coordination, monooxy bridging coordination, dioxygen bridging coordination and so on.[14–16] Isonicotinic acid (HIA) is a very good organic ligand, because both ends of its structure contain a carboxyl group and a nitrogen atom respectively, which can make it achieve different coordination geometry and extended structure with metal ions.

Based on the interest in this aromatic carboxylic acid ligand and the author's region is rich in yttrium element. In order to better develop the use of yttrium element, our research group prepared a novel dual-core type of yttrium-isonicotinic acid coordination complexes $[Y(HIA)_3(H_2O)_2]_n \cdot nYCl_3$ (HIA = isonicotinic acid).

2. Experimental

2. 1. Materials and Physical Measurements

All chemicals are analytical reagent grade, commercially obtained and used without further purification. Photoluminescence experiment was carried out on a F97XP photoluminescence spectrometer. The solid-state UV/Vis measurements were conducted on TU1901 UV/Vis spectrometer with the wavelength range of 200–900 nm. The infrared spectra was obtained from the PE Spectrum-One Fourier transform infrared (FT-IR) with the wavelength range of 4000–500 nm.

2. 2. Preparation of the Title Complex $[Y(HIA)_3(H_2O)_2]_n \cdot nYCl_3$

$YCl_3 \cdot 6H_2O$ (1 mmol, 304 mg), isonicotinic acid (1 mmol, 123 mg) and 15 mL distilled water were loaded into a 25 mL Teflon-lined stainless steel vessel, then heated to 453 K and kept there for seven days in an oven, and finally cooled down to room temperature. Yellow block-like crystals were collected manually and washed with distilled water. Yield = 56% (based on $YCl_3 \cdot 6H_2O$). IR (KBr, cm^{-1}): 3451 (vs), 2924 (w), 2855 (w), 1620 (vs), 1546 (w), 1413 (m), 766 (w), 530 (w), as shown in Figure 1.

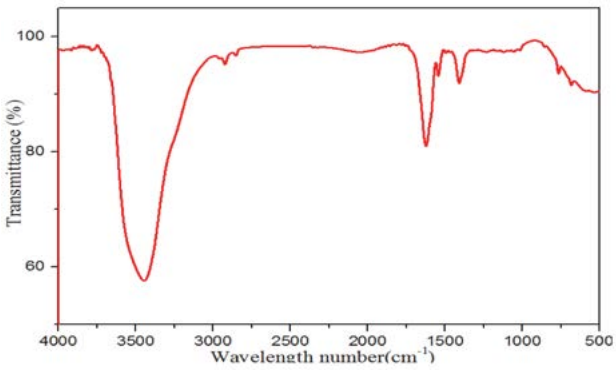

Figure 1. FTIR spectra of the title complex $[Y(HIA)_3(H_2O)_2]_n \cdot nYCl_3$

2. 3. Crystallographic Data Collection and Refinement

The single crystal data of the title complex were collected with a suitable single crystal (size 0.03 mm, 0.05 mm, 0.16 mm) on a SuperNova charge-coupled device (CCD) X-ray diffractometer. During the data acquisition, the crystal temperature was kept at 293(2) K. Using Olex2, the structure was solved with the SIR2004 structure solution program using Direct Methods and refined with the ShelXL refinement package using Least Squares minimisation.[17–19] All of the non hydrogen atoms were generated based on the subsequent Fourier difference diagram and were refined anisotropically. The hydrogen atoms were located theoretically and ride on their parent atoms. Table 1 provides a summary of the crystallographic data and refinement results. Table 2 lists selected bond lengths and angles for the title complex.

Table 1. Crystallographic data and structure analysis for the title complex

Empirical formula	$C_{18}H_{16}Cl_3N_3O_8Y_2$
Formula weight	686.51
Temperature/K	293(2)
Crystal system	triclinic
Space group	*P*-1
a/Å	9.6260(3)
b/Å	11.8097(4)
c/Å	14.6020(5)
α/°	101.772(3)
β/°	95.383(3)
γ/°	113.606(3)
V/Å^3	1460.28(9)
Z	2
ρ_{calc}g/cm^3	1.561
μ/mm^{-1}	4.269
F(000)	676.0
Crystal size/mm^3	0.16 × 0.05 × 0.03
Radiation	MoKα (λ = 0.71073)
2θ range for data collection/°	7.53 to 50.048
Index ranges	$-11 \le h \le 11$, $-13 \le k \le 14$, $-17 \le l \le 11$
Reflections collected	11237
Independent reflections	3901 (R_{int} = 0.0346)
Data/restraints/parameters	3901/273/318
Goodness-of-fit on F^2	1.011
Final R indexes [$I>=2\sigma(I)$]	R_1 = 0.0692, wR_2 = 0.1735
Final R indexes [all data]	R_1 = 0.0771, wR_2 = 0.1831
Largest diff. peak/hole / e Å^{-3}	1.03/–0.60

3. Results and Discussion

3. 1. Crystal Structure

The title complex crystallizes in the triclinic *P*-1. The asymmetric unit contains two neutral molecules $Y(HIA)_3 \cdot (H_2O)_2$ and YCl_3, as shown in Figure 2. The yttrium ions have two different coordination environments. The Y(1) ion is coordinated with three oxygen of three isonicotinic acid and two oxygen of two water, forming a slightly distorted tetragonal antiprism configuration, the Y(2) ion is surrounded by three chloride ions. The 1-*D* chains are interconnected through Y(1) bridges running along the *a* axis, as shown in Figure 3. In the title complex, the following bond distances were observed: Y(1)-O(1W) / O(2W) / O(1)^2 / O(2) / O(3) / O(4)^3 / O(5)^3 / O(6) 2.609(8) / 2.625(7) / 2.510(6) / 2.444(7) / 2.522(7) / 2.449(7) / 2.842(8) / 2.452(7) Å; Y(2)-Cl(1A)^1 / Cl(2) / Cl(3) 3.153(4) / 2.780(3) / 2.716(3) Å; Cl(1A)-Y(2)

2.776(5) Å; Cl(1A)-Y(2)[1] 3.153(4) Å; Cl(1B)-Y(2) 2.748(5) Å, as shown in Table 2. These are comparable with those reported in the literature for similar or related compounds.[20–22]

In the title complex, there are 5 groups of intermolecular hydrogen bonds and one group of intramolecular hydrogen bonds in the crystal structure of the form O-H···O / N and C-H···O, as shown in Table 3 and Figure 4 for details. In the crystal structure, the nitrogen atom does not directly participate in coordination, but undergoes intermolecular hydrogen bonding with O-H. There is no π···π interaction, but it has a large number of intermolecular hydrogen bonds and van de Waals attraction yielding the 3-*D* supramolecular structure running parallel to the *bc* plane, and the crystal packing is presented in Figure 5.

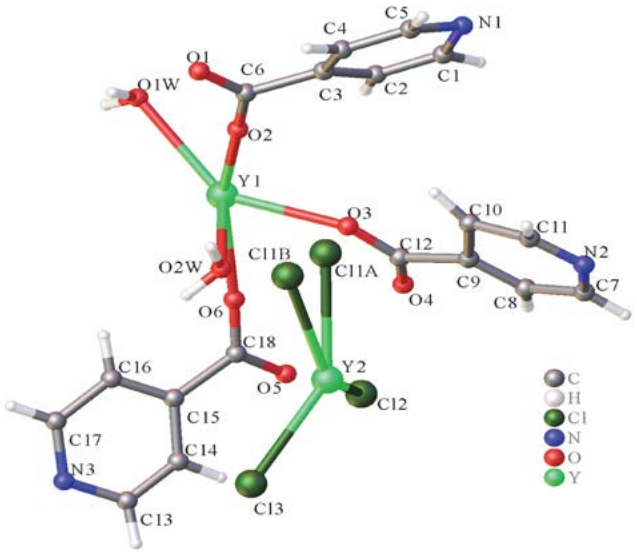

Figure 2. The asymmetric unit molecular diagram of the title complex

3. 2. Hirshfeld Surface analysis

In order to further analyze various weak intermolecular forces, the Hirshfeld surface analysis method was

Table 2. Selected bond lengths (Å) and bond angles (°) for the title complex

Atom-Atom	Lengths(Å)	Atom-Atom	Lengths(Å)
Cl(1A)-Y(2)	2.776(5)	Y(1)-O(3)	2.522(7)
Cl(1A)-Y(2)[1]	3.153(4)	Y(1)-O(4)[3]	2.449(7)
Cl(1B)-Y(2)	2.748(5)	Y(1)-O(5)[3]	2.482(8)
Y(1)-O(1W)	2.609(8)	Y(1)-O(6)	2.452(7)
Y(1)-O(2W)	2.625(7)	Y(2)-Cl(1A)[1]	3.153(4)
Y(1)-O(1)[2]	2.510(6)	Y(2)-Cl(2)	2.716(3)
Y(1)-O(2)	2.444(7)	Y(2)-Cl(3)	2.780(3)
Atom-Atom-Atom	Angle (°)	Atom-Atom-Atom	Angle (°)
Y(2)-Cl(1A)-Y(2)[1]	94.26(13)	O(4)3-Y(1)-O(6)	69.7(3)
O(1W)-Y(1)-O(2W)	123.5(2)	O(5)3-Y(1)-O(1W)	70.8(3)
O(1)2-Y(1)-O(1W)	72.1(3)	O(5)3-Y(1)-O(2W)	137.5(3)
O(1)2-Y(1)-O(2W)	72.1(3)	O(5)3-Y(1)-O(1)[2]	142.1(3)
O(1)2-Y(1)-O(3)	138.0(3)	O(5)3-Y(1)-O(3)	79.0(3)
O(2)-Y(1)-O(1W)	72.6(3)	O(6)-Y(1)-O(1W)	136.9(3)
O(2)-Y(1)-O(2W)	72.0(2)	O(6)-Y(1)-O(2W)	77.6(2)
O(2)-Y(1)-O(1)[2]	99.5(2)	O(6)-Y(1)-O(1)[2]	82.3(2)
O(2)-Y(1)-O(3)	79.1(2)	O(6)-Y(1)-O(3)	78.3(2)
O(2)-Y(1)-O(4)[3]	143.0(3)	O(6)-Y(1)-O(5)[3]	121.3(2)
O(2)-Y(1)-O(5)[3]	76.5(2)	Cl(1A)-Y(2)-Cl(1A)[1]	85.74913)
O(2)-Y(1)-O(6)	147.3(2)	Cl(1A)-Y(2)-Cl(3)	133.2(2)
O(3)-Y(1)-O(1W)	142.4(3)	Cl(1B)-Y(2)-Cl(3)	109.3(3)
O(3)-Y(1)-O(2W)	67.6(2)	Cl(2)-Y(2)-Cl(1A)[1]	112.79(18)
O(4)3-Y(1)-O(1W)	71.9(3)	Cl(2)-Y(2)-Cl(1A)	110.7(2)
O(4)3-Y(1)-O(2W)	138.9(3)	Cl(2)-Y(2)-Cl(1B)	131.9(2)
O(4)3-Y(1)-O(1)[2]	79.4(3)	Cl(2)-Y(2)-Cl(3)	110.12(6)
O(4)3-Y(1)-O(3)	126.1(2)	Cl(3)-Y(2)-Cl(1A)[1]	98.8(2)
O(4)3-Y(1)-O(5)[3]	82.2(3)		

Symmetry codes: 1 = 3 – *x*, 2 – *y*, – *z*; 2 = 3 – *x*, 2 – *y*, 1 – *z*; 3 = 4 – *x*, 2 – *y*, 1 – *z*.

Table 3. Hydrogen bond lengths (Å) and bond angles (°)

D-H···A	[ARU]	D-A(Å)	H···A(Å)	D···A(Å)	D-H···A(°)
O(1W)-H(1WA)···O(2)	[2876]	0.86	2.55	3.195(12)	132
O(1W)-H(1WA)···O(2W)	[2876]	0.86	2.10	2.862(13)	148
O(2W)-H(2WA)···N(3)	[2986]	0.86	1.99	2.775(12)	152
O(2W)-H(2WB)···O(1W)	[2876]	0.85	2.03	2.862(13)	165
C(14)-H(14)···O(5)		0.93	2.57	2.875(15)	100
C(16)-H(16)···O(1)	[2876]	0.93	2.43	3.338(15)	164

Symmetry codes: [2876] = 3 – *x*, 2 – *y*, 1 – *z*; [2986] = 4 – *x*, 3 – *y*, 1 – *z*.

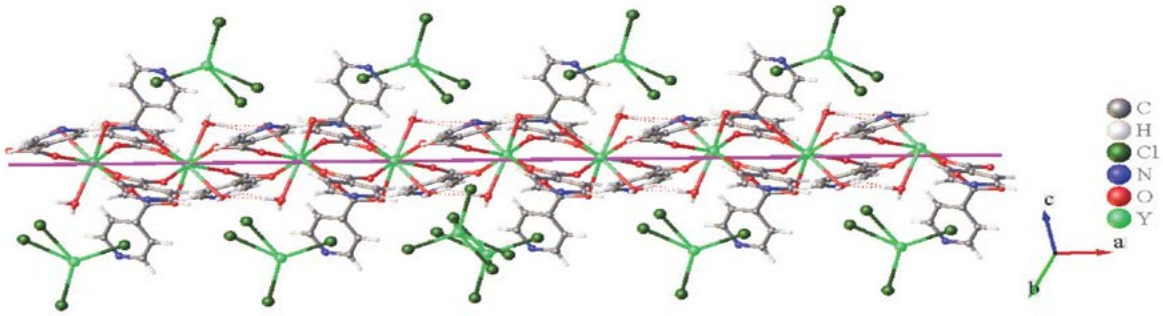

Figure 3. The 1-D chain-like structure of the title complex viewed along the *a* axis.

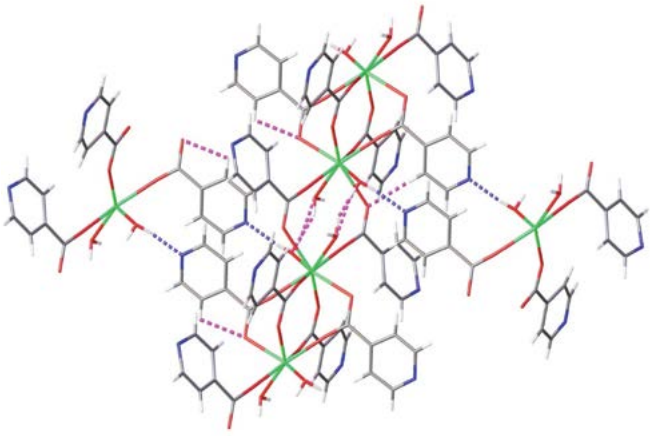

Figure 4. The hydrogen bond diagram of the title complex. n[YCl_3] molecules not involved in the motif show were removed for clarity.

used to quantitatively analyze the weak intermolecular forces of the title complex. Through Crystal Explorer 3.1 program calculation of the Hirshfeld Surface of the complex molecules distribution of force, obtaining dnorm, shape index, and curvature figure. Hirshfeld analysis was performed on the title complex, as shown in the Figure 6. The range of dnorm, shape index and curednes is –1.0523 ~ 1.9122, –1.0000 ~ 1.0000, –4.0000 ~ 4.0000.

The Hirshfeld surface of the title complex and the contribution percentage of various mode of action to the Hirshfeld surface are shown in Figure 7. The four main mode of action are H···H, C···H, O···H and H···Cl connections. Among them, the effect of H···H is distributed in the middle area of the fingerprint, which contributes the most to the Hirshfeld surface, reaching 25.7%, and is the most important mode of action. Next are the action of C···H,

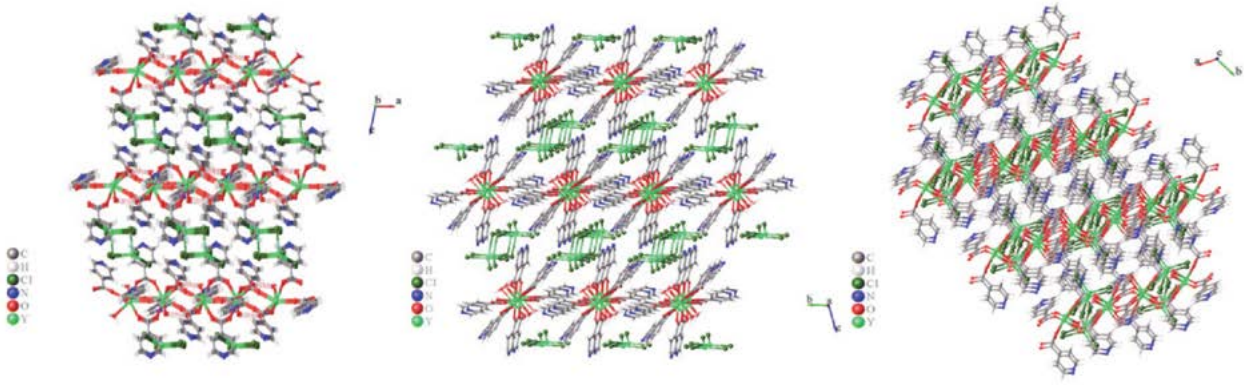

Figure 5. The packing diagram of the title complex viewed along the *ab,bc, bc.*

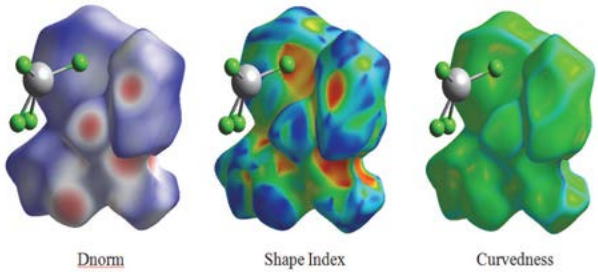

Figure 6. The Hirshfeld surface picture of the title complex

H···Cl and O···H, with a contribution ratio of 14.1%, 14.1% and 13.6%, respectively.

3. 3. Solid-State Photoluminescence Spectra

In order to investigate the photoluminescence characteristics of the title complex, the photoluminescence spectra of the solid state samples were measured at room temperature, and the results are shown in Figure 8. It is obvious that the photoluminescent spectrum of the title complex displayed an effective energy absorption in a

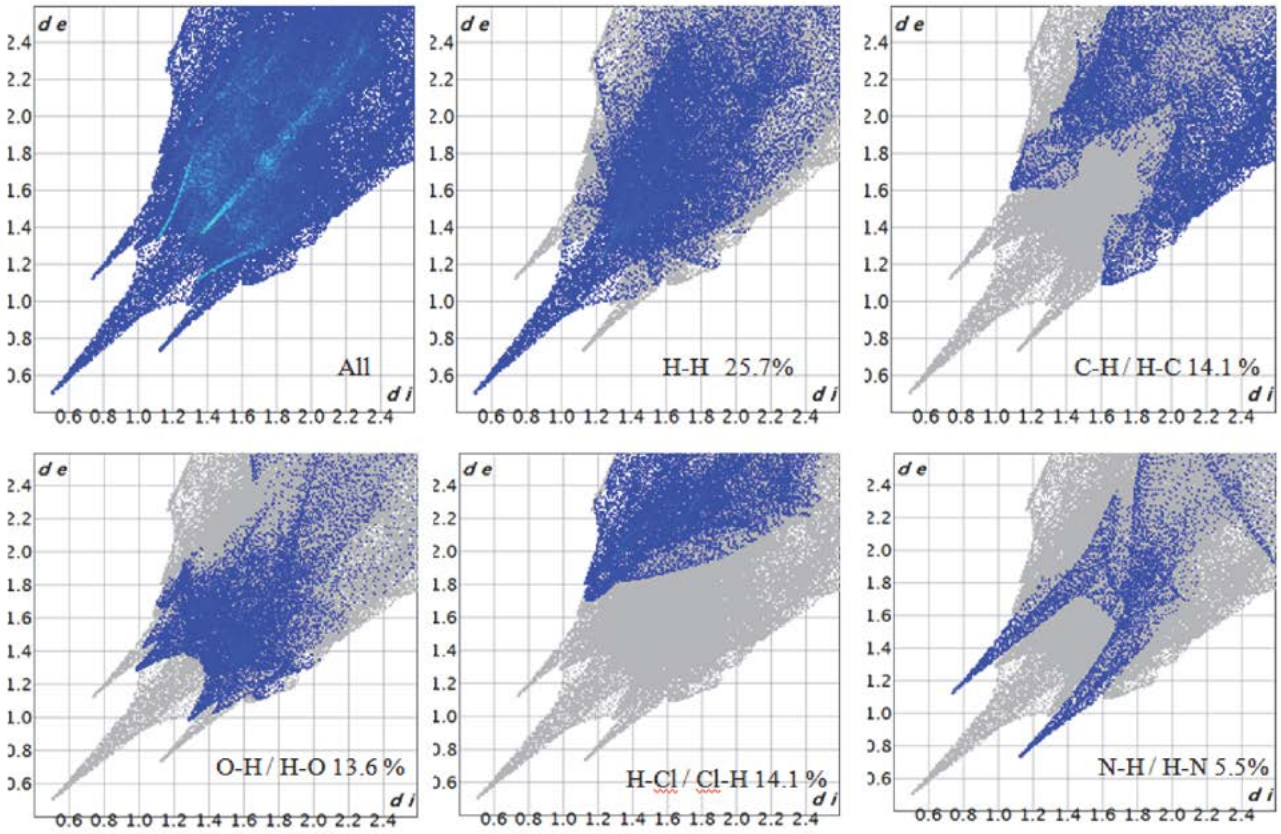

Figure 7. 2D fingerprint of the title complex (global 2D fingerprint & fingerprint of different molecular connections)

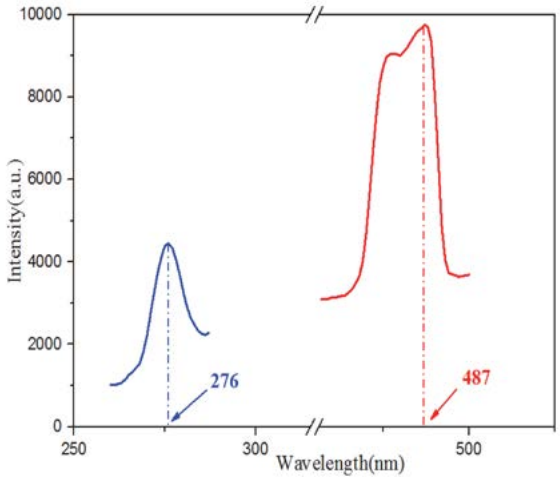

wavelength rang of 350–500 nm. Upon the emission of 487 nm, the excitation spectrum showed a band at 276 nm. Upon excitation at 276 nm, the emission spectrum was characterized by a sharp band at 487 nm in the blue region. The emission band of the title complex located in the blue violet light region with the CIE1931 chromaticity coordinate (0.1049, 0.1221), as shown in Figure 8. As the result, the title complex is a potential blue photoluminescent material.

Figure 8. Solid-state photoluminescence of the title complex (blue line: emission; red line: excitation).

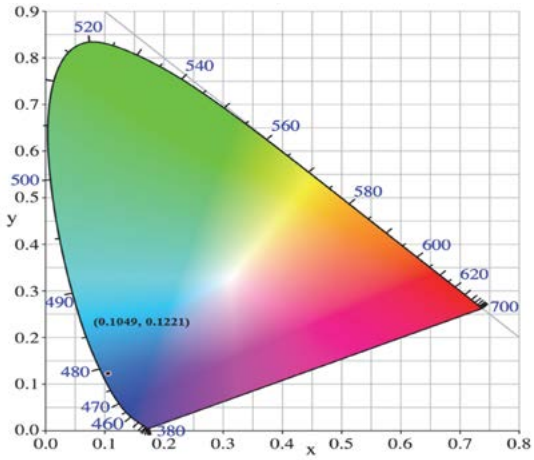

Figure 9. The CIE chromaticity diagram and chromaticity coordinate of the emission spectrum of the title complex

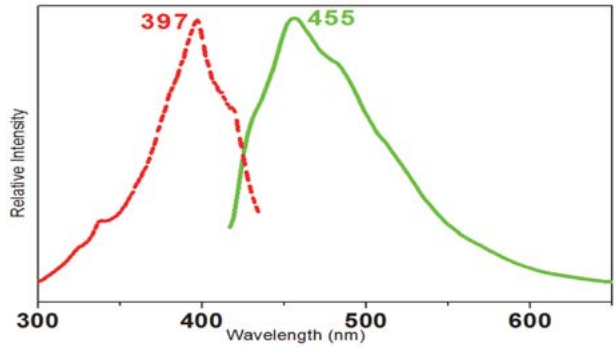

Figure 10. Solid-state photoluminescence of the title HIA ligand (red line: emission; green line: excitation).

It can be seen from the solid-state fluorescence spectra of Figure 8 and Figure 10 that the emission peak of the ligand HIA is 455 nm under the excitation peak of 397 nm. However, under the excitation peak of 276 nm, the emission peak of the title yttrium complex is a single peak of 487 nm, with a red shift of 32 nm relative to the HIA ligand. This is mainly due to the electronic transition and stacking effect inside the ligand.

3. 4. Solid-State UV-Vis Diffuse Reflectance Spectra of the Title Complex

Based on barium sulfate as the reference for 100% reflectivity, the UV-Vis diffuse reflectance spectra of the title complex was measured at room temperature, using the solid-state compound. The Kuberka-Monk function $\alpha/S = (1\text{-}R)^2/2R$ is used to process the solid diffuse reflection spectral data, where the parameter α refers to the absorption coefficient, *S* is the scattering coefficient which is actually independent of the wavelength when the particle size is larger than 5 μm, and *R* is the reflectivity. By extrapolating the linear part of the α/*S* absorption edge with the energy graph, the value of the optical band gap can be determined.[23,24] Solid UV-Vis diffuse reflection spectrum shows that the title complex possesses a wide optical band gap of 2.03 eV, as shown in Figure 11. Therefore, this may be a good candidate material for broad band gap semiconductors, which is obviously larger than those of GaAs (1.4 eV), CdTe (1.5 eV), and $CuInS_2$ (1.55 eV), which are called efficient band gap photovoltaic materials.[25,26]

4. Conclusions

In summary, a novel yttrium complex with isonicotinic acid (HIA) ligand including lattice water and yttrium chloride molecule has been synthesized and characterized by single-crystal X-ray diffraction. The title yttrium complex is characterized by a one-dimensional chain-like structure by metal ion bridge chain bond, the title yttrium complex packs for form a layer structure including weak interactions containing hydrogen bonding and van de Waals attraction. Based on the solid-state photoluminescent spectrum and the solid-state diffuse reflectance spectrum experiment, we believe that the title complex may be a good blue photoluminescent material (CIE chromaticity coordinates 0.1049, 0.1221) and a candidate material for wide band gap semiconductor (2.03 eV).

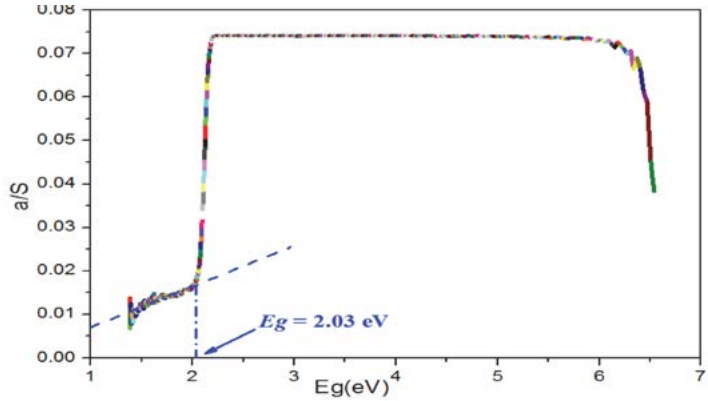

Figure 11. Solid-state UV/Vis diffuse reflectance spectrum of the title complex.

Supplementary Materials

Crystallographic data for the structural analysis have been deposited with the Cambridge Crystallographic Data Center, CCDC **No. 2190846**. Copies of this information can be obtained free of charge from the Director, CCDC, 12 Union Road, Cambridge, CBZ, 1 EZ, UK (fax: +44-1223-336033); email: deposit@ccdc.cam.ac.uk or online at http://www.ccdc.cam.ac.uk.

Acknowledgements

The National Natural Science Foundation of China (22168018), the Natural Science Foundation of Jiangxi Province of China (20232BAB203048, 20202BABL203003), the Science and Technology Plan Project of Ji'an (20211-025317).

Data Availability

Data Availability CCDC **2190846** contain the supplementary crystallographic data for the title complex. The data can be obtained free of charge from the Cambridge Crystallographic Data Centre via www.ccdc.com.ac.uk/structures.

Declarations

Conflict of interest on behalf of all authors, the corresponding author states that there is no conflict of interest.

5. References

1. P. Xu, J. Li, J. H. Huang, F. Yu, C. H. Li, Y. X. Zheng, *New J. Chem.* **2021**, *45*, 13168-13174. **DOI:**10.1039/D1NJ02454J
2. S. Chorazy, M. Wyczesany, Sieklucka, *Molecules* **2017**, *22*, 1902. **DOI:**10.3390/molecules22111902
3. Y. Abbas, S. N. Yun, M. S. Javed, J. G. Chen, M. F. Tahir, Z. Q. Wang, et al., *Ceram. Inter.* **2020**, *46*, 4470-4476. **DOI:**10.1016/j.ceramint.2019.10.173
4. A. Quader, G. M. Mustafa, S. K. Abbas, H. Ahmad, S. Atiq, *Chem. Eng. J.* **2020**, *396*, 125198. **DOI:**10.1016/j.cej.2020.125198
5. D. Mahmoud, M. S. EI-Deab, M. E. Elshakre, N. K. Allam, *J. Phys. Chem. C* **2020**, *124*, 7007-7015. **DOI:**10.1021/acs.jpcc.9b12045
6. J. N. Xing, M. Shu, W. Y. Wang, R. Zhang, J. Liu. *Chin. J. Inorg. Chem.* **2021**, *37*, 1847-1852.
7. W. T. Chen. *J. Mol. Struct.* **2020**, *1219*, 128580/1-128580/6. **DOI:**10.1016/j.molstruc.2020.128580
8. W. A. Fu, H. J. Chen, Y. Y. Han, W. Y. Wang, R. Zhang, J. Liu. *New J. Chem.* **2021**, *45*, 19082-19087. **DOI:**10.1039/D1NJ04074J
9. H. Shi, F. F. Zhao, X. H. Chen, S. L. Yang, J. N. Xing, H. J. Chen, et al. *Tetrahedron Lett.* **2019**, *60*, 151330-151334. **DOI:**10.1016/j.tetlet.2019.151330
10. H. J. Chen, G. Y. Lyu, Y. F. Yue, T. W. Wang, D. P. Li, H. Shi, et al. *J. Mat. Chem. C* **2019**, *7*, 7249-7259. **DOI:**10.1039/C9TC01520E
11. J. H. Wei, J. W. Yi, M. L. Han, B. Li, S. Liu, Y. P. Wu, et al. *Chem - Asian J.* **2019**, 14, 3694-3701. **DOI:**10.1002/asia.201900706
12. X. W. Li, N. Ma, G. T. Xu, R. Zhang, J. Liu. *Sol. Energy Mater. Sol. Cells* **2022**, *234*, 111449. **DOI:**10.1016/j.solmat.2021.111449
13. C. Jeffrey, R. B. David, L. Li, L. M. David. *J. Biomed. Opt.* **2019**, *24*, 051409-051420.
14. H. H. Chen, X. G. Yi, C. W. Pan, J. W. Wen, C. Zhang. *Chin. J. Struct. Chem.* **2021**, *4*, 501-506.
15. X. G. Yi, Y. Z. Liu, X. N. Fang, X. Y. Zhou, Y. X. Li. *Chin. J. Struct. Chem.*, **2019**, *38*, 325-330.
16. W. Y. Wang, H. J. Chen, Y. F. Yue, R. Zhang, J. Liu. *Dyes Pigm.* **2021**, *194*, 109615. **DOI:**10.1016/j.dyepig.2021.109615
17. O. V. Dolomanov, L. J. Bourhis, R. J. Gildea. *J. Appl. Crystallogr.* **2009**, *42*, 339-341. **DOI:**10.1107/S0021889808042726
18. G. M. Sheldick. *Acta Crystallogr. A,* **2008**, *64*, 112-122. **DOI:**10.1107/S0108767307043930
19. G. M. Sheldrick. *Acta Crystallogr C,* **2015**, *71*, 3-8. **DOI:**10.1107/S2053273314026370
16. H. R. Rong, X. M. Wang, Y. W. Ma, G. X. Gao, H. Q. Su, L. F. Lai, Q. Liu. *Chin. J. Inorg. Chem.* **2021**, *37*, 206-212.
17. X. G. Yi, F. P. Lai, Y. Y. Yan, C. Zhang, W. P. Li. *J. Chem. Res.* **2021**, *45*, 295-304. **DOI:**10.1177/1747519820948363
18. Y. N. Wang, S. D. Wang, K. Z. Cao, G. D. Zou. *J. Photochem. Photobiol., A* **2021**, *411*, 113204. **DOI:**10.1016/j.jphotochem.2021.113204
19. X. N. Fang, X. G. Yi, Z. Q. Yi, J. Y. Chen, Y. X. Li. *Chin. J. Inorg. Chem.* **2019**, *35*, 930-936.
20. K. Lou, F. H. Zu, J. J. Yi, C. M. Cui. *Organometallics* **2021**, 40, 4092-4097. **DOI:**10.1021/acs.organomet.1c00501
21. T. F. Jenkins, S. Bekoe, J. W. Ziller, F. Furche, W. J. Evans. *Organometallics* 2021, 40, 3917-3925. **DOI:**10.1021/acs.organomet.1c00482
22. C. H. Li, Y. F. Kuang, W. Li, Y. L. Li. *Chin. J. Struct. Chem.* 2020, *39*, 2016-2020.
23. W. B. Fan, Y. R. Jiang, T. Xu, Z. Li, L. J. Chen. *Mater. Rep. B* **2015**, 29, 15-20.
24. Y. Zhu, H. F. Jiu, B. J. Gao, H. L. Zuo. *J. North Univ. China, Nat. Sci. Ed.* **2008**, 29, 347-351. **DOI:**10.1007/s11741-008-0412-4
25. W. S. Lin, H. M. Kuang, H. Luo, W. T. Chen. *Chin. J. Struct. Chem.* **2019**, 38, 1012-1020.
26. S. K. Loyalka, C. A. Riggs. *Appl. Spectrosc.* **1995**, *49*, 1107-1110. **DOI:**10.1366/0003702953964976
27. C. Lee, W. Yang, R. G. Parr. *Phys. Rev. B* **1988**, *37*, 785-789. **DOI:**10.1103/PhysRevB.37.785

28. W. Bensch, P. Dürichen, O. Helmer, A. Reller, U. Sazama. *Inorg. Chim. Acta* **1996**, *252*, 47-53.
DOI:10.1016/S0020-1693(96)05297-8

Povzetek

S hidrotermalno reakcijo smo sintetizirali nov itrijev kompleks $[Y(HIA)_3(H_2O)_2]_n \cdot nYCl_3$ (HIA = izonikotinska kislina) in ga karakterizirali z monokristalno rentgensko difrakcijo. Spojina ima enodimenzionalno (1-*D*) verižno strukturo. Fotoluminiscenčne meritve v trdnem stanju kažejo na močan emisijski vrh pri 487 nm, ki ga lahko pripišemo karakterističnemu elektronskemu prehodu v ligandu. Spojina kaže CIE (Commission Internationale de I' Éclairage) kromatske koordinate v modrem področju (0.1049, 0.1221). Meritve UV/Vis v trdnem stanju so pokazale na širino prepovedanega 2.03 eV.